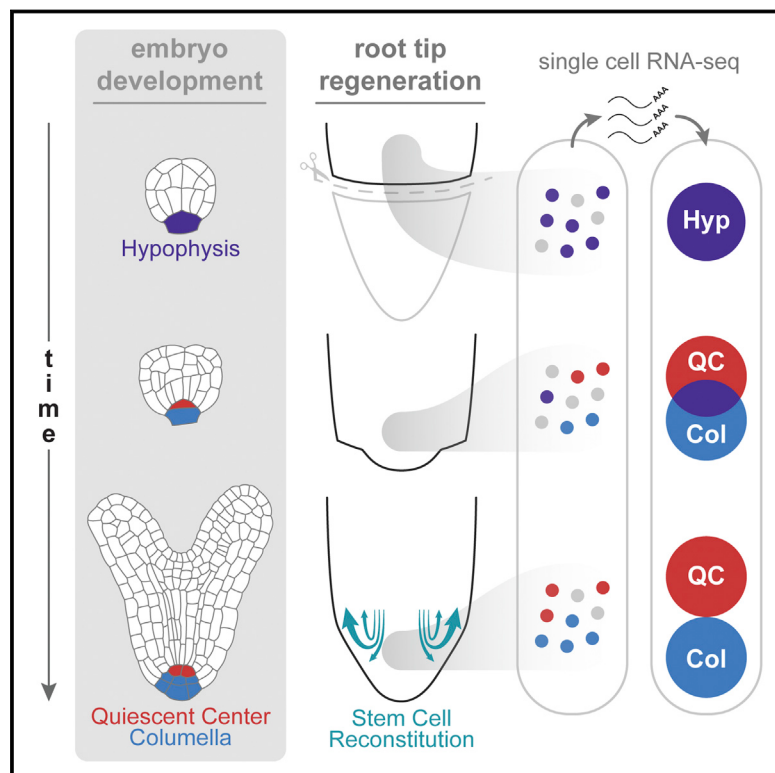


# Root Regeneration Triggers an Embryo-like Sequence Guided by Hormonal Interactions

## Graphical Abstract



## Highlights

- Removal of root stem cells triggers their reformation from multiple remnant tissues
- Stem cell reformation is preceded by embryonic-like development sequence
- Antagonistic hormonal signaling domains position regenerated tissues and stem cells

## Authors

Idan Efroni, Alison Mello, Tal Nawy, ...,  
Ashley Powers, Rahul Satija,  
Kenneth D. Birnbaum

## Correspondence

[ken.birnbaum@nyu.edu](mailto:ken.birnbaum@nyu.edu)

## In Brief

Plants have dramatic regenerative capacity, including replacement of their stem cell niche after its complete excision. In a process that recapitulates the steps of embryogenesis, many specialized, transit-amplifying cells can reform stem cells. Complementary hormonal domains provide the spatial cues that play a role in patterning new tissue boundaries and a new stem cell niche.

## Accession Numbers

GSE74488

# Root Regeneration Triggers an Embryo-like Sequence Guided by Hormonal Interactions

Idan Efroni,<sup>1,3</sup> Alison Mello,<sup>1</sup> Tal Nawy,<sup>1</sup> Pui-Leng Ip,<sup>1</sup> Ramin Rahni,<sup>1</sup> Nicholas DelRose,<sup>1</sup> Ashley Powers,<sup>2</sup> Rahul Satija,<sup>1,2</sup> and Kenneth D. Birnbaum<sup>1,\*</sup>

<sup>1</sup>Center for Genomics and Systems Biology, Department of Biology, New York University, New York, NY 10003, USA

<sup>2</sup>New York Genome Center, New York, NY 10013, USA

<sup>3</sup>Present address: The Robert H. Smith Institute of Plant Sciences and Genetics in Agriculture, The Hebrew University, Rehovot 76100, Israel

\*Correspondence: [ken.birnbaum@nyu.edu](mailto:ken.birnbaum@nyu.edu)

<http://dx.doi.org/10.1016/j.cell.2016.04.046>

## SUMMARY

Plant roots can regenerate after excision of their tip, including the stem cell niche. To determine which developmental program mediates such repair, we applied a combination of lineage tracing, single-cell RNA sequencing, and marker analysis to test different models of tissue reassembly. We show that multiple cell types can reconstitute stem cells, demonstrating the latent potential of untreated plant cells. The transcriptome of regenerating cells prior to stem cell activation resembles that of an embryonic root progenitor. Regeneration defects are more severe in embryonic than in adult root mutants. Furthermore, the signaling domains of the hormones auxin and cytokinin mirror their embryonic dynamics and manipulation of both hormones alters the position of new tissues and stem cell niche markers. Our findings suggest that plant root regeneration follows, on a larger scale, the developmental stages of embryonic patterning and is guided by spatial information provided by complementary hormone domains.

## INTRODUCTION

Plants have a wide capacity to regenerate their organs after damage by re-establishing regions of growth and patterning known as meristems (Sugimoto et al., 2011). Remarkably, excision of most of the root meristem, including the entire stem cell niche and its supporting cells (the quiescent center; QC), triggers rapid regeneration and resumption of normal growth (Figure 1A; Feldman, 1976; Sena et al., 2009). Here, we ask what kind of repair system can restore the root tip's growth and tissue organization after its complete removal.

Since the stem cell niche is removed with root tip excision, it cannot initiate the regeneration process. However, regeneration may rely on other potent cell types in the remaining stump (Birnbaum and Sánchez Alvarado, 2008; Sugimoto et al., 2011). In particular, the pericycle cell layer has organogenetic capacity and is the source of lateral roots in the adult (Lavenus et al., 2013). Further, under some conditions, it can generate a partially organized pluripotent tissue known as callus (Atta et al., 2009;

Sugimoto et al., 2010), suggesting that the pericycle may serve as a dormant stem cell niche that supports regeneration after damage (Sugimoto et al., 2011). However, plant cells are known to be plastic, and lineage studies show that cells throughout the root meristem can readily change their fate according to their position (Kidner et al., 2000). Furthermore, while lateral roots are formed from the pericycle, adventitious roots can form from cambium and other vasculature-associated cells (Bellini et al., 2014). Thus, an alternative model for regeneration is that missing tissues and stem cells regenerate from any remnant meristematic cell, guided by positional cues.

Tissue repatterning may occur either through the activation of regeneration-specific mechanisms or by the “recapitulation” of stereotypical organogenesis (Sánchez Alvarado and Tsionis, 2006). In animals, there is evidence that embryonic gene expression programs and developmental processes are reiterated during regeneration (Chen et al., 2014; Kikuchi et al., 2010; Roensch et al., 2013). Similarly in plants, regeneration is accompanied by activation of key developmental regulators that function in embryogenesis and adult root formation (Kareem et al., 2015; Sena et al., 2009; Xu et al., 2006). However, it is unclear how closely, or whether at all, the sequence of early development events is recapitulated during regeneration.

Many plant growth and patterning processes are regulated by the interaction between the phytohormones auxin and cytokinin (Schaller et al., 2015). During embryonic root formation, the two hormones form complementary domains, and perturbation of the signaling pathway of either hormone leads to embryonic root defects (Hamann et al., 2002; Hardtke and Berleth, 1998; Müller and Sheen, 2008). Classic studies demonstrated the importance of the balance between these hormones during in vitro regeneration (Skoog and Miller, 1957), but how this balance mediates tissue formation during regeneration is not well known.

Here, we dissected the early stages of regeneration by combining lineage and marker analysis with gene expression profiling in regenerating cells. We show that new root tissue is formed by the activity of newly specified stem cells recruited from multiple tissues in the remaining stump, ruling out the activity of a cryptic stem population drawn exclusively from pericycle cells. Activation of the new niche is preceded by rapid identity transitions and a sequence of developmental events that closely resembles embryonic root formation. Furthermore, regeneration was impaired in mutants with embryonic root defects but not in mutants that specifically perturbed lateral root development.

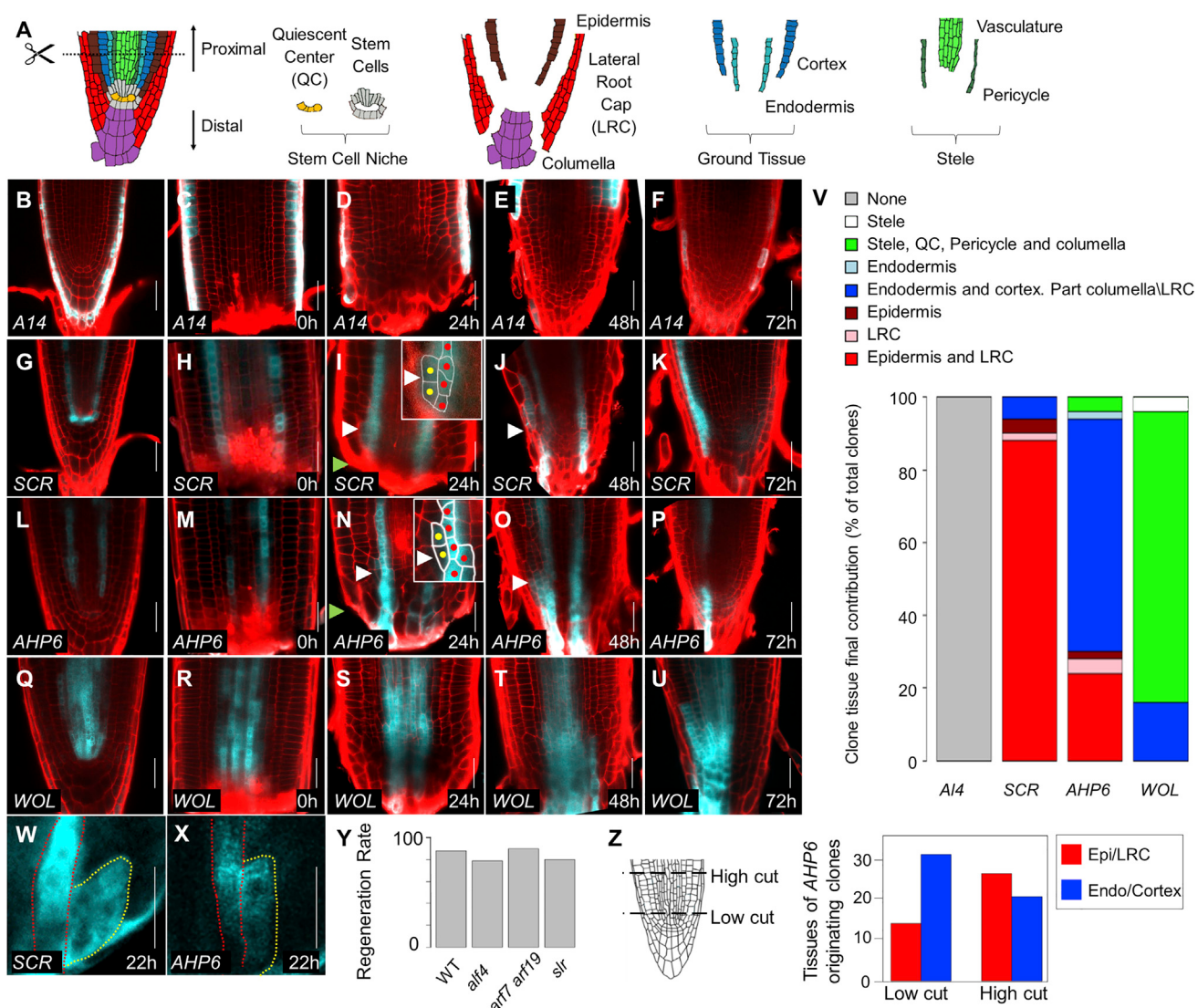


**Figure 1. Growth Dynamics during Root Tip Regeneration**

(A) Schematic representation of root meristem organization. Dotted line marks the cut site used in the study.

(B–U) Confocal images of tissue-specific clones induced using the promoters *A14* (B–F), *SCR* (G–K), *AHP6* (L–P), and *WOL* (Q–U) before (B, G, L, and Q) and immediately after (C, H, M, and R) root cutting and at 24 hpc (D, I, N, and S), 48 hpc (E, J, O, and T), and 72 hpc (F, K, P, and U). Red channel indicates propidium iodide staining of cell walls. White arrowheads mark the presumed location of a new stem cell. Green arrowheads mark the cut site. Insets show magnified view of nascent clones. Red and yellow dots mark cells from original clone and new divisions, respectively.

(V) Proportions of the target tissues in fully regenerated tip for each of the clonal lines.

(W and X) Part of a time series tracking clones in live roots. Red line marks the original clone; yellow line marks new growth. See full series in [Figure S1](#).

(Y) Regeneration rate of mutants in lateral root production. No significant difference was detected. WT, wild-type.

(Z) The identity of clones derived from an *AHP6* marked tissue at 72 hpc from cuts at two different heights. High cuts produced more epidermal clones than low cuts ( $\chi^2$  test;  $n = 98$ ;  $p = 0.014$ ).

Scale bars, 20  $\mu$ m.

See also [Figure S1](#).

We further show that altering the auxin and cytokinin domains during a narrow time window causes a coordinated change in the position of multiple root tissues and the stem cell niche. The results suggest that the interaction between these hormones sets up positional information for early tissue patterning and stem cell niche formation and that early events in embryogenesis are replayed within a different cellular organization.

## RESULTS

### The Root Regenerates by De Novo Stem Cell Niche Formation from Multiple Tissues

To test the different models of regeneration and track the contributions of multiple tissues to root tip regeneration, we generated a lineage-tracking system that permanently marks a selected

tissue upon induction by dexamethasone (*promoter>>CRE:GR 35S:lox-terminator-lox-CFP*). Plants carrying lineage constructs for different radial tissues were grown for 5 days, induced for 24 hr, checked for robust tissue-specific expression, and then cut and transferred to non-inductive plates. At least 100 plants were examined for each tissue of origin (Figures 1B–1V).

Clones generated using the A14 promoter (AT5G43040; Lee et al., 2006), marking the outer layer of the root (Figures 1B and 1C), did not contribute to the regenerating tip and were pushed upward as the new root tip formed (Figures 1D–1F and 1V). Interestingly, clones generated using the endodermal SCR promoter (Figures 1G and 1H) mostly produced lineages that occupied the positions of the new epidermis and lateral root cap (LRC; Figures 1I–1K and 1V), overlapping with the *WER* epidermal/LRC identity marker (Figure S1A). The endodermal clones were continuous with regenerating cells in the epidermal position and converged near the cut site (Figure 1I). Lateral cell divisions characteristic of epidermis/LRC stem cells (Bennett and Scheres, 2010) were observed at this position as early as 24 hr post-cut (hpc; Figure 1I), suggesting that an endodermal cell assumed a stem cell identity to generate the new epidermal layer. We verified these endodermis-derived epidermal stem-cell-like divisions by live imaging clones over time (Figure 1W; Figure S1B) and by tracking cell division patterns in live roots over 68 hr (Movie S1).

To test whether the pericycle plays a special role in root tip regeneration, we induced and tracked clones using the *AHP6* promoter, which marks the xylem pole pericycle and protoxylem (Figures 1A, 1L, and 1M). The *AHP6*-marked clones mostly produced cells occupying the position of the new cortex/endodermis tissues (Figures 1N–1P and 1V), generated by stem-cell-like divisions at 24 hpc (Figures 1N, 1X, and S1C). These cells produced tissue-specific clones until they were replaced by unmarked cells around 72 hpc (Figure 1P). In contrast to lateral root formation (Figure S1D), the contribution of the *AHP6*-marked clone was limited and did not comprise all new cells of the root tip. Thus, it is unlikely that root tip regeneration is driven by a lateral root initiation program. As further support, root regeneration frequency was unaffected in mutants severely impaired in the production of pericycle-derived lateral roots or callus (*arf4-1* [Sugimoto et al., 2010] 79%, n = 49; *arf7 arf19* [Okushima et al., 2007] 90%, n = 20; *slr* [Fukaki et al., 2002] 80%, n = 50), as compared to wild-type (88%, n = 100; Figure 1Y).

The coordinated activation of stem-cell-like divisions at 24 hpc suggested that a new niche may be formed at this time point. Indeed, clones generated using the stele-specific *WOL* promoter (Figures 1Q–1U; Mähönen et al., 2000) gave rise to new distally growing columella cells, indicating re-establishment of the characteristic bidirectional growth of the niche (Bennett and Scheres, 2010; Figures 1S–1U), with cells in the QC position eventually displacing the surrounding stem cells (Figure 1U; Heyman et al., 2013; Kidner et al., 2000). Overall, these transitions indicate that almost all prior cell identities were competent to form new stem cells.

The broad cell identity transformations rule out a strict model in which remnant cells in the proximal meristem repopulate like identities. However, the different distributions of identity transitions (Figure 1V) may suggest that tissues have restricted

competence to take on new fates. To test the role of competence over relative position, we cut the root at two different locations along the tapering tip. The width of the stele and endodermis is  $37 \pm 2 \mu\text{m}$  just above the QC but is  $56 \pm 5 \mu\text{m}$  at  $80 \mu\text{m}$  above the QC, due to greater cell numbers in the stele (n = 16; Figure 1Z), so that cuts at these locations alter the position of the pericycle in relation to the root center. In agreement with broad competence for fate change, we observed a shift in the identity of clones originating from the *AHP6* lineage (Figure 1Z; n = 98; p = 0.0135,  $\chi^2$  test).

Overall, our results reveal that the new root tip is derived from a small population of cells, recruited from multiple tissues, which begin to act in a coordinated stem-cell-like manner by 24 hpc. These broad fate transitions are guided by the cells' relative position in the remnant tissue.

### Injury Triggers a Gradual Loss of Proximal Identity Near the Cut Site

To map cell identity transitions, we tracked multiple tissue markers during regeneration. Endodermal marker *SCR:YFP* (Wysocka-Diller et al., 2000) and stele marker *WOL:GFP* were lost near the cut site by 6–12 hpc, receding to about three cell rows above the cut site by 16 hpc (Figures 2A and 2B). The stele recession was confirmed by the loss of xylem marker *S4* and phloem marker *S32* (Lee et al., 2006; Figures S2A–S2F). In contrast, expression of the outer layer markers *WER* and *GL2* remained relatively stable (Figure 2C; Figures S2G–S2I; Lee and Schiefelbein, 1999; Lin and Schiefelbein, 2001). Also, the inner endodermal expression of the ground tissue marker *J0571* receded more than its outer cortical domain (Figure 2D), capturing a demarcation point in the clearing of cell identities.

Interestingly, while stem-cell-like divisions were observed at 24 hpc, expression of cell identity markers did not initially correlate with this activity. Also, although stem cell activity resumed in an inside-out manner, endodermal (*SCR*) and epidermal (*WER*) markers began to recover their expression pattern in an outside-in pattern starting at 30 hpc, only fully recovering their normal expression in the stem cells by 48 hpc (Figures 2B and 2C). Similarly, the stele marker *SHR* (Helariutta et al., 2000) only regained its proper distal nuclear localization at 48 hpc (Figure 2E). Curiously, in some cases, expression of a small discontinuous *SCR* domain was visible at the center of the stele.

Together with the identity transitions observed using clonal analysis, these results implicate a dome-shaped region of ~40 cells at the center of the stump as the site of re-patterning. Both the proximodistal and the radial axes of the root were reset near the cut site (Figure 2F). Cell identity recovered in the direction opposite to stem cell growth, separating the reactivation of stem cells from cell identity respecification.

### Single-Cell Transcriptomics Reveal Rapid Identity Transitions

To characterize the transcriptional dynamics in the region of reorganization, we used single-cell RNA sequencing (RNA-seq) to profile individual stele cells from induced *WOL* and *AHP6* clones in uncut and regenerating roots at three time points: 3 hpc, the earliest time point we could collect; 16 hpc, prior to

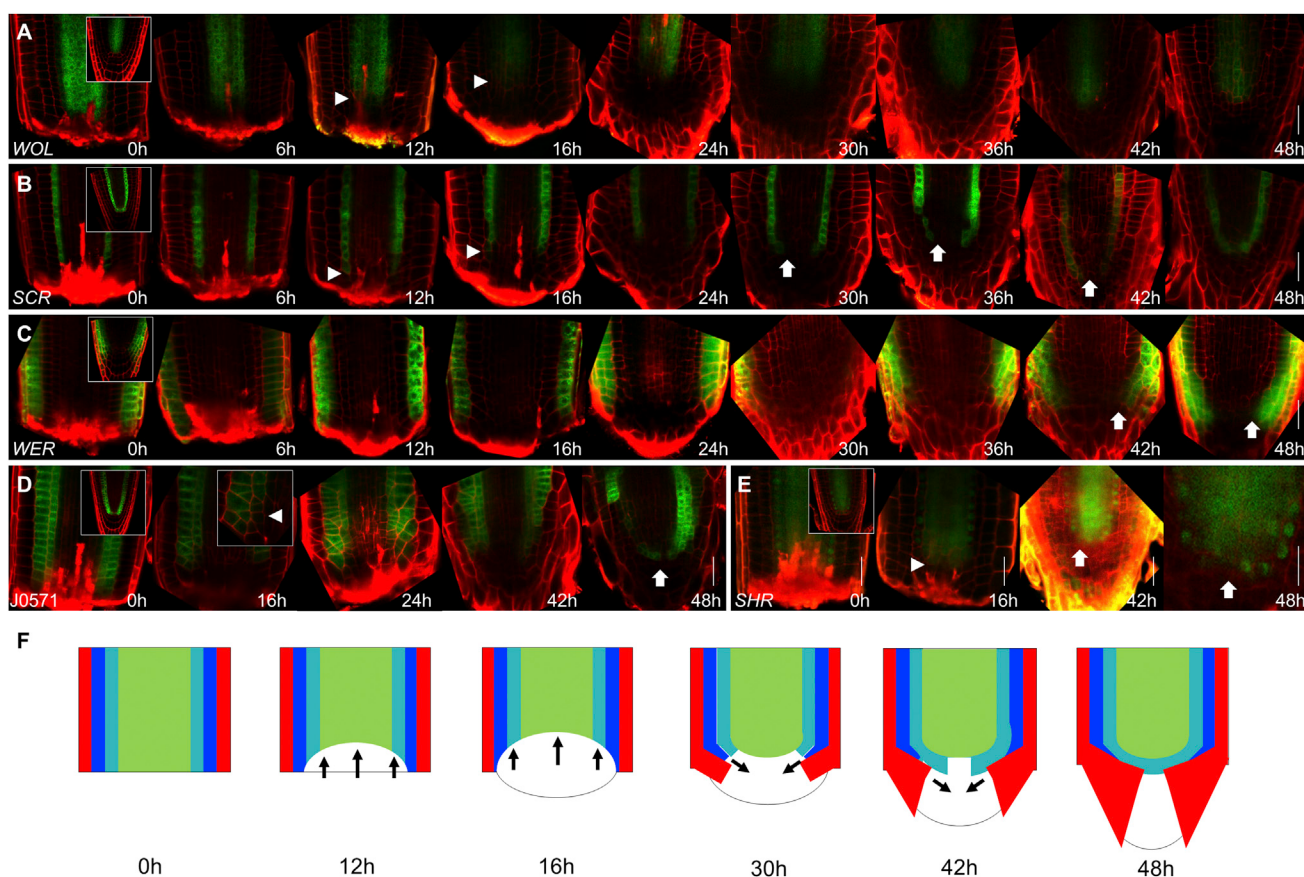


**Figure 2. Dynamics of Loss and Recovery of Proximal Identities**

(A–E) Confocal images of *WOL*:GFP (A), *SCR*:YFP (B), *WER*:GFP (C), J0571 (D) and *SHR*:*SHR*:GFP (E) during regeneration. Insets at 0 hr show uncut roots. Arrowheads mark the receding edge of the proximal identity markers. Arrows mark recovery of identity markers. Inset at (D) 16 hpc shows a high magnification of the identity recession region.

(F) Illustration summarizing identity transition during regeneration. Red indicates epidermis/LRC, blue indicates cortex, cyan indicates endodermis, and green indicates stele. Arrows indicate the directions of identity recession and recovery.

Scale bars, 20  $\mu$ m.

See also Figure S2.

stem cell niche activation; and 46 hpc, following the recovery of root growth. Cells were collected from dissociated meristems by cell sorting with stringent gates to ensure droplets with only one fluorescent cell, followed by mRNA amplification and sequencing using a modified version of the SMART-Seq2 protocol (Satija et al., 2015).

Cells were classified using the Index of Cell Identity (ICI) algorithm, which can identify stable and transitional fates using single-cell expression data (Birnbaum and Kussell, 2011; Efroni et al., 2015). We used a reference dataset of 579 identity marker genes (Tables S1 and S2) to classify cells into 14 root tissue types (Figure S3A; Table S3), which we grouped as stele, QC, columella, epidermis/LRC, and ground tissue (Figures 3A–3D).

We collected 238 cells, of which 74% could be classified into at least one reference identity. As expected for *WOL* and *AHP6* marked cells, most (116/177) were classified as stele (Figures 3A–3D). However, some cells lost their stele identity and gained distal identities as early as 3 hpc (Figure 3B). This rapid change in identity is consistent with the observed recession of stele

markers near the cut site. The transitioning stele cells scored a surprising mixture of QC, columella, and epidermis/LRC—identities that are either removed by cutting (QC and columella) or are normally absent from internal root tissue (epidermis/LRC). Multidimensional scaling grouped the transdifferentiating cells together, regardless of their tissue of origin (*WOL* or *AHP6*), suggesting that cells from different tissue sources converged to a single identity (Figure S3B). The lack of residual stele identity suggested that the mixed-identity cells originated from the tip of the stump, where stele markers were lost (Figures 2D, S2A, and S2B). As regeneration progressed, cells with distinct distal identities, such as QC and columella alone, became more common (Figures 3C and 3D). Consistent with the clonal analysis, stele-derived cells contributed mainly to the new columella and QC but also to some of the LRC and ground tissue (Figure 1V).

Thus, single-cell analysis revealed a rapid change from stele to mixed distal cell identities, which gradually separated into columella and QC during regeneration. This developmental sequence resembles the dynamics of embryonic root formation,

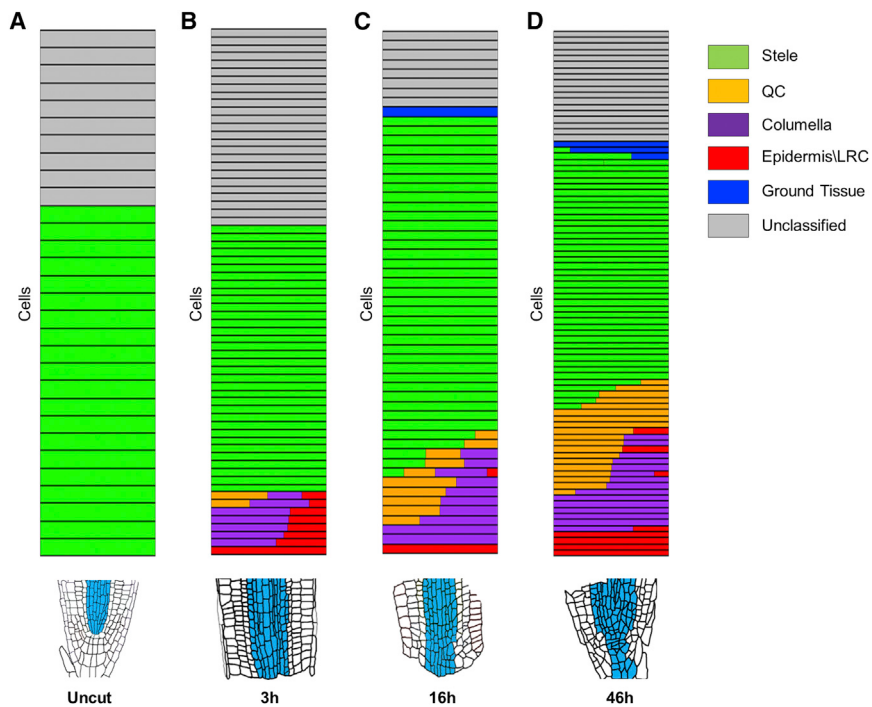


**Figure 3. Identity of Single Cells Isolated from Regenerating Roots**

(A–D) Relative cell identity in individual cells isolated from uncut roots (A) and at 3 hpc (B), 16 hpc (C), and 46 hpc (D). Each row represents a single cell. Identity is shown as a color-coded bar consisting of the normalized ICI score for each tissue type. Multiple color bars in a single row indicate mixed identity within a single cell. Blue sectors in root illustrations (bottom) represent the domains from which single cells were isolated.

See also Figure S3.

proximal identity loss (Figures 4E–4J). Between 16 hpc and 48 hpc, *WOX5* marked a proximal domain, and *WIP4* marked a distal domain (Figures 4K–4N; Figures S4C–S4H). Similarly, the hypophysis-expressed marker *IAA10* (Rademacher et al., 2012), which is confined to the columella in the adult (Figure S4I), overlapped with the *WOX5* domain at 16 hpc but then separated into a distal domain (Figures S4J and S4K). Thus, much like the embryo, these three markers overlap in hypophysis-like cells

that appear early in regeneration and subsequently separate into distinct domains.

To rule out generally promiscuous expression of QC and columella markers, we examined plants bearing *WOX5:mCherry* and *PET111*, which marks differentiated columella (Figure S4L). *PET111* never overlapped with *WOX5* and was not detected until proximal-distal domain separation at 24 hpc (Figures S4M–S4O).

During hypophysis division, the transcription factor *TARGET OF MONOPTEROS7* (*TMO7*) is expressed in the provascular cells above the hypophysis and moves distally into the hypophysis cell to regulate its division (Schlereth et al., 2010). Analysis of the transcriptional reporter *TMO7:GFP-NLS*, the translational reporter *TMO7:TMO7-GFP*, and the non-mobile protein fusion *TMO7:TMO-GFPx3* showed that, following tip removal, expression of *TMO7* is lost in the stump region by 16 hpc, when mixed-distal cell identities were detected in the same domain, while the *TMO7* protein moves into that region from the surrounding cells (Figures 4O–4W). The rapid recovery of this pattern further supports the existence of a hypophysis-like state during early stages of regeneration.

Next, we used genetic perturbation to test the shared program between embryonic root formation and regeneration. Mutants in *JACKDAW* (*JKD*) form a normal embryonic root but fail to maintain expression of QC markers in the adult (Figures S4P and S4Q; Welch et al., 2007). Consistent with an activation of an embryonic phase of root development, expression of the QC marker *WOX5* was re-activated during the regeneration of *jkd* mutants (Figures S4R and S4S) but diminished when the tip was fully regenerated (Figures S4T and S4U).

We also tested the regeneration frequency in mutants that exhibit a failure in hypophysis division and subsequently lacked an embryonic root: single mutants in the auxin response

during which a single cell—the hypophysis—expresses multiple distal identity markers before dividing to generate distinct QC and columella progenitors (Crawford et al., 2015; ten Hove et al., 2015; Müller and Sheen, 2008; Scheres et al., 1994).

### Recovery of Distal Fates Resembles an Embryonic Developmental Sequence

We explored the similarity of regeneration to embryonic root formation by examining the expression of hypophysis-expressed genes (Crawford et al., 2015; Rademacher et al., 2012; Ueda et al., 2011; Wysocka-Diller et al., 2000) in regenerating roots. These genes generally displayed a gradual upregulation in the mixed-identity cells between 3 hpc and 16 hpc and became differentially expressed as QC and columella identities became distinct (Figure 4A), a pattern we corroborated using a recently identified set of genes expressed in the basal meristem and hypophysis (Wendrich et al., 2015; Figure S4A). In contrast, genes expressed in stages of embryogenesis prior to hypophysis division or that regulate the embryonic formation of other tissues were not induced in the mixed cells (Figure 4B), indicating the activation of a hypophysis-specific rather than a general embryonic program. Hypophysis-expressed genes were consistently upregulated in mixed-identity cells at 3 hpc and 16 hpc, but their expression was diminished by 46 hpc (Figure S4B), further supporting the existence of a transient hypophysis-like state during regeneration.

To understand the spatial dynamics of distal identity separation, we analyzed reporters that are co-expressed in the hypophysis: *WOX5:GFP*, which subsequently marks the QC, and *WIP4*, which later marks both the QC and columella (Figures 4C and 4D; Crawford et al., 2015; Haeger et al., 2004; Nawy et al., 2005). Starting at 6 hpc, both markers were co-expressed within the region of

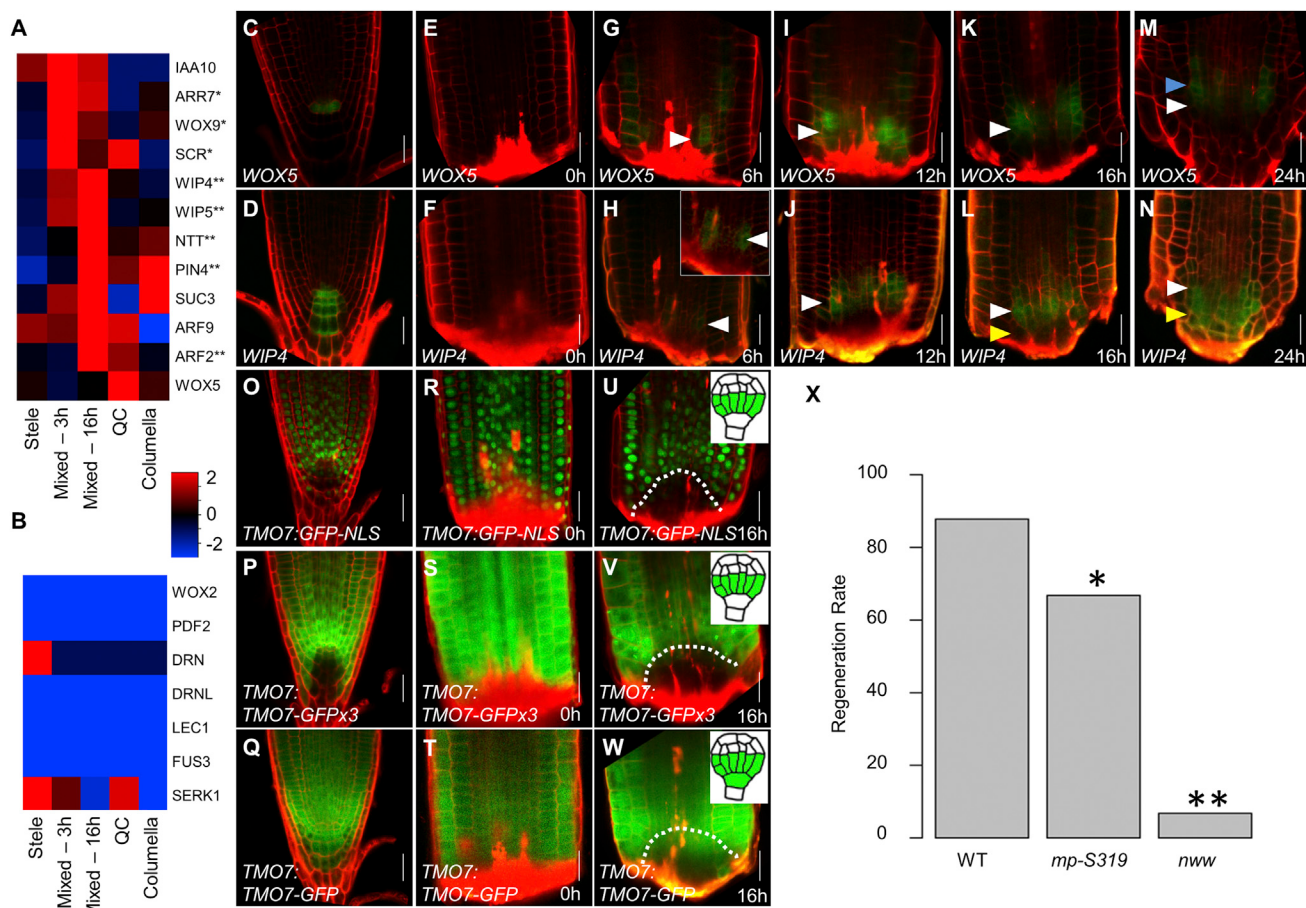


**Figure 4. Proximodistal Domain Separation Resembles Embryonic Hypophysis Division**

(A and B) Mean expression values of known hypophysis (A) or embryonic but non-hypophysis (B) expressed genes in single cells grouped according to their identity. One and two asterisks indicate significant upregulation at 3 hr and 16 hr, respectively ( $p < 0.05$ , Wilcoxon test).

(C–N) Confocal images of *WOX5* (C, E, G, I, K, and M) and *WIP4* (D, F, H, J, L, and N) reporters over the first 24 hr of regeneration. Blue, white, and yellow arrowheads mark the forming proximal, overlapping, and distal domains, respectively. Inset shows magnified and gain-enhanced GFP signal.

(O–W) Confocal images of transcriptional (O, R, and U) and translational non-mobile (P, S, and V) and mobile (Q, T, and W) reporters of *TMO7*. Inset at 16 hr shows the embryonic expression of each reporter. Dotted line marks the region of identity loss.

(X) Regeneration rate of mutants defective in hypophysis division. WT, wild-type. \* $p = 0.02$ ; \*\* $p < 1E-10$ ;  $\chi^2$  test. Scale bars, 20  $\mu$ m.

See also Figure S4.

factor *MONOPTEROS* (*MP*) and triple mutants of the *NO TRANSMITTING TRACT* gene family (*NWW*; Crawford et al., 2015; Hamann et al., 1999; Hardtke and Berleth, 1998). In the weak *mp-S319* allele, ~10% of seedlings fail to form an embryonic root, but those that escape exhibit normal growth (Schlereth et al., 2010; De Smet et al., 2010). The escaped *mp-S319* adult roots showed a 25% reduction in the frequency of regeneration compared to wild-type. The *nww* mutants form an embryonic root in only 2.5% of plants but can be rescued with a transient auxin treatment and then grow without supplemental auxin (Crawford et al., 2015). These rescued *nww* mutant roots had a 92% reduction in regeneration (wild-type: 88%,  $n = 100$ ; *mp-S319*: 66%,  $n = 21$ ,  $\chi^2$  test,  $p = 0.02$ ; *nww*: 7%,  $n = 15$ ,  $\chi^2$  test, and  $p < 1E-10$ ; Figure 4X). Thus, both mutant phenotypes are consistent with a reliance on the early phases of embryonic root formation during regeneration.

### Hormone and Tissue Markers Follow Embryonic Dynamics

In the embryo, the signaling domains of the phytohormones auxin and cytokinin briefly overlap in the hypophysis before they separate into a proximal cytokinin and a distal auxin domain (Müller and Sheen, 2008). In an apparent recapitulation of the overlap of the two hormones, rapid response genes for cytokinin (*ARR* family; To et al., 2004) and auxin (*AUX/IAA* family; Chapman and Estelle, 2009) were coordinately upregulated in single chimeric cells during the early stages of regeneration (Figure 5A).

To follow the spatial dynamics of this interaction, we used the cytokinin response reporter *TCSn:GFP* (*TCSn*; Zürcher et al., 2013) and the auxin response reporters *DR5rev:GFP* (Friml et al., 2003) and fast-maturing *DR5rev:3xVENUS-N7* (Heisler et al., 2005). In uncut roots, *TCSn* is expressed in the stele and root cap but is absent from proximal tiers of the columella

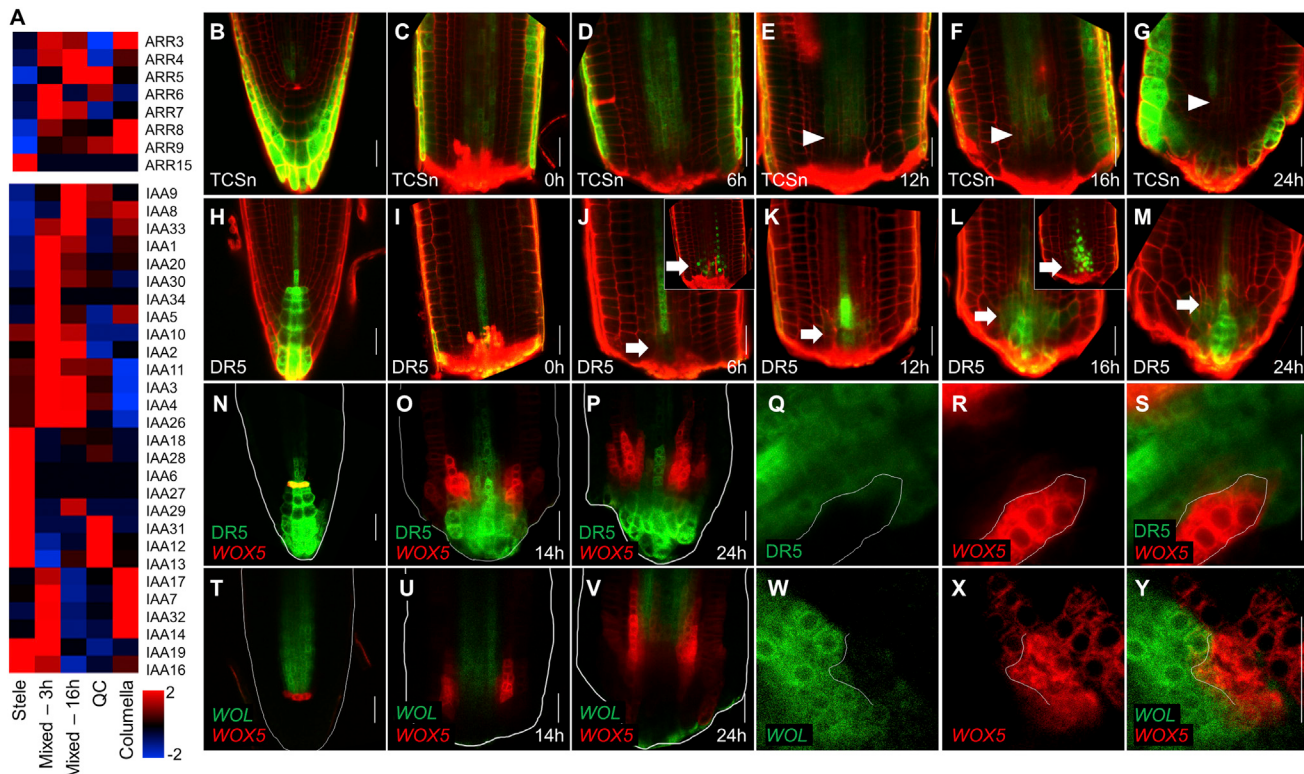


**Figure 5. Expression of Hormonal Response Markers during Proximodistal Domain Separation**

(A) Mean expression values in single cells, grouped by identity, of A-class *ARR* (top) or *AUX/IAA* (bottom) gene families.  
(B–M) Expression of the cytokinin marker TCSn (B–G) and auxin marker DR5 (H–M) during regeneration. Arrowheads mark the recession of the TCSn signal. Arrows mark induction of DR5. Insets in (J) and (L) show expression of the rapid maturing *DR5rev:NLS-3xVenus* at the corresponding time points.  
(N–P) Dual-marker expression of DR5 (green) and WOX5 (red) before cutting (N) and at 14 hpc (O) or 24 hpc (P).  
(Q–S) An invading sector of WOX5 (red) expression in the DR5 (green) domain in single channel (Q and R) and overlay (S) at 14 hpc.  
(T–Y) Confocal image of WOL (green) and WOX5 (red) plants before cut (T) and at 14 hpc (U) and 24 hpc (V), including high magnification of a WOX5-invading sector (W–Y) at 14 hpc.  
Scale bars, 20  $\mu$ m.

See also Figure S5.

(Figure 5B; Bishopp et al., 2011; Zürcher et al., 2013). At 6 hpc, the remnant TCSn expression in the stele remained unchanged (Figures 5C and 5D), gradually receding proximally at later time points (Figures 5E–5G). The distal auxin maximum (Figure 5H) was completely excised during the removal of the tip, leaving only low expression in immature xylem cells (Figure 5I). However, auxin signaling was rapidly induced in a region of stele near the cut site, as shown by *DR5rev:3xVENUS-N7* expression (Figures 5J and 5L, inset; Figures S5A–S5E), creating a transient overlap with the cytokinin reporter (Figures 5D–5G and 5J–5M). Thus, the embryonic dynamics of the two hormones—initial overlap, followed by separation into distinct proximal cytokinin and distal auxin domains—were recapitulated during root tip regeneration.

In the adult root, *WOX5* expression is restricted to the QC, whose location overlaps with and depends upon a local maximum of auxin signaling (Sabatini et al., 1999; Xu et al., 2006). In contrast, embryonic *WOX5* expression begins in the hypophysis, but after hypophysis division, it shifts proximally away from the auxin maximum (Müller and Sheen, 2008). Regeneration in *DR5:GFP WOX5:mCherry* roots (Figure 5N) showed that, after

a brief overlap (compare *WOX5* in Figure 4G and *DR5* in Figure 5J at 6 hr), *WOX5:mCherry* expression shifted proximally, and the two markers then remained mutually exclusive (Figures 5O and 5P), exhibiting an embryonic expression pattern.

In addition, the patterns were highly suggestive of regulatory relationships. For example, *WOX5* and *DR5* expression were almost always in mutually exclusive domains when in close proximity (Figures 5Q–5S). Mutually exclusive expression was also often detected between *WOX5* and the cytokinin receptor *WOL* (Figures 5T–5Y), suggesting that an interaction between hormone signaling and cell-identity markers may guide patterning during regeneration.

### Auxin-Cytokinin Interaction Guides the Establishment of the Proximodistal and Radial Axes

Both cytokinin and auxin are required for proper formation of the embryonic root, but the role of their interaction is not clear. It was suggested that an auxin domain positions the nascent root embryonic meristem, as mutations in *HANABA TARANU* (*HAN*) that cause a proximal shift and a lateral shift in the embryonic auxin

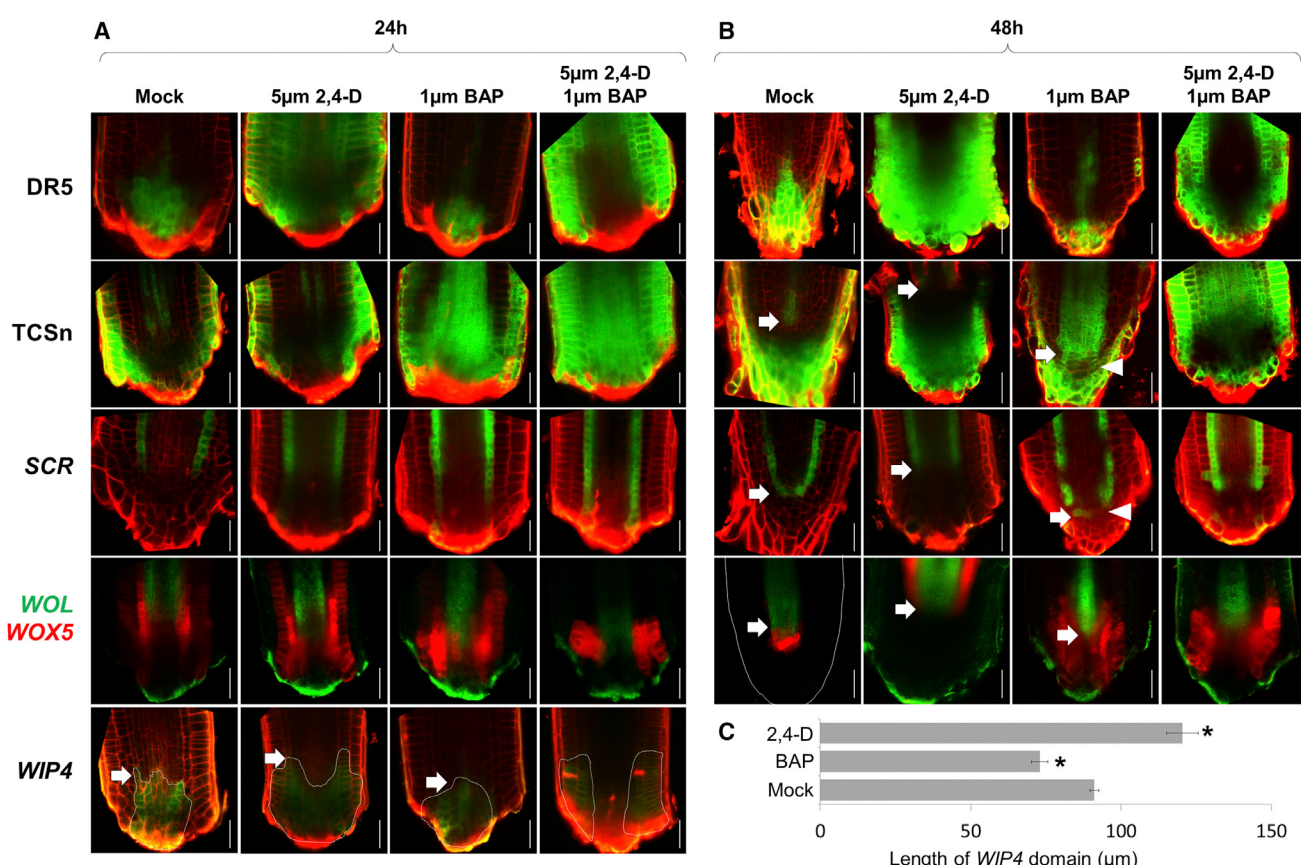


**Figure 6. Effects of Hormone Treatment on Meristem Patterning**

(A and B) Confocal images of mock-, 2,4-D-, BAP-, or 2,4-D-and-BAP-treated regenerating roots at 24 hpc (A) and 48 hpc (B). Arrows mark proximodistal shifts in position of markers compared to mock-treated control. Arrowheads mark sporadic cytokinin signaling expansion and concomitant loss of *SCR* expression. (C) Length of *WIP4* domain at 24 hpc under different treatments. Error bars indicate SE. n = 8 for each treatment. Asterisk indicates significant difference compared with mock (Student's t test, p < 1E-4 for BAP, and p < 1E-3 for 2,4-D).

Scale bars, 20 μm.

See also Figure S6.

domain also led to a corresponding shift in the expression of distal root markers, including the QC marker *WOX5* (Nawy et al., 2010). Interestingly, we saw a similar phenomenon during regeneration in the *han-16* mutant, where, at 16 hpc, *WOX5* occupied a more proximal and lateral domain than wild-type (Figure S6A; Student's t test, p = 0.02), indicating that hormonal domains may influence tissue specification similarly both during embryogenesis and regeneration. Therefore, we sought to determine whether hormone domains could guide tissue positioning in the regeneration process.

Application of the auxin analog 2,4-D caused expansion of the DR5 signal and a proximal recession of the TCSn signal by 48 hpc (Figures 6A and 6B). In accordance, endodermal and stele markers were expressed in a more proximal position than normal (Figure 6B; Figure S6B), with *SCR* converging at 72 hpc (Figures S6C and S6D). Strikingly, expression of the distal marker *WIP4* was significantly expanded proximally, bounded by an internal stele/cytokinin domain (Figures 6A and 6C). Our results indicate that auxin treatment causes a coordinated proximal shift in the auxin-cytokinin border that is accompanied by a

coordinated shift in the position of the border between the radial cell files and the cap.

Treatment with cytokinin during regeneration diminished the DR5 domain while causing distal and lateral expansion of the TCSn reporter (Figures 6A and 6B). Under these conditions, expression of *SCR* recovered in a more distal position than normal, invading the cap region (Figure 6B). In agreement, the domains of the stele markers *WOL* (Figure 6B) and *SHR* (Figure S6E) stabilized at a more distal position than in control plants. Finally, the distal shift in markers coincided with a reduction in the *WIP4* domain size (Figures 6A and 6C), showing that cytokinin application caused a coordinated distal shift in the position of root tissues. To examine the effects of cytokinin treatment on the position of the stem cell niche, we allowed cytokinin-treated plants of the *SCR* lineage line to recover on hormone-free media for 24 hr. In agreement with the general shift in tissue positioning, we observed that the epidermal stem cell formed at an abnormal distal position (Figure S6F).

We could cause a more dramatic alteration of hormone domains with a dual auxin-cytokinin treatment, which displaced

the auxin domain to the flank of the root stump (**Figures 6A** and **6B**). Accordingly, the *WIP4* domain was displaced to a lateral position (**Figure 6A**). Strikingly, *SCR* and *SHR* domains now expanded outward in a radial direction (**Figure 6B**; **Figure S6G**), suggesting that hormonal interaction can also pattern the radial axis of the root meristem. Indeed, cytokinin treatment by itself caused a patchy loss of *SCR* (**Figure 6B**; **Figure S6H**) with the *TCSn* domain exhibiting a complementary patchy expansion (**Figure 6B**).

Interestingly, the effect of hormone treatment on patterning was limited to a narrow early time window, as the same treatments at 24 hpc or on intact roots had little effect on patterning (**Figures S6I–S6P**). Indeed, a similar narrow window for hormonal response was shown for the embryo (Müller and Sheen, 2008). Thus, the results show that the embryo-like juxtaposition of auxin-cytokinin domain acts early to set up the position where cell files will converge and the stem cell niche will eventually form. Overall, we conclude that root regeneration involves the de novo formation of the root axis using the same developmental sequence as during embryonic root formation, its position being guided by hormone domains and their interactions.

## DISCUSSION

### Regeneration through Activation of Embryonic Organogenesis Programs

A fundamental question in regeneration biology is that of “recapitulation,” or whether organ regeneration in the adult follows similar programs as those used during embryonic development (Sánchez Alvarado and Tsonis, 2006). Here, we show that the regeneration of the root tip initiates in an embryonic-like sequence of distal root meristem formation, followed by the activation of a stem cell niche that propagates the root. We have previously reported that the root tip can regenerate even in mutants in which the stem cell niche failed to be maintained in the adult root (Sena et al., 2009). However, these mutants could all properly form an embryonic root (Aida et al., 2004; Sabatini et al., 2003), while rescued *nww* mutants, which have a functional root meristem, recapitulated the severe embryonic root formation defects when cut. The association between embryonic and regenerative processes is also evident in the regeneration of adventitious roots, where *mp* mutants had reduced capacity to form these roots, and *gnom* mutants, which are also defective in embryonic root development, could not form them at all (Berleth and Jürgens, 1993; Mayer et al., 1993).

An interesting aspect of root tip regeneration is that, in contrast to the embryo, where the proximal-distal separation involved two cells, the same separation in the root occurs on a larger spatial scale. However, the overall mechanistic similarity between these processes suggests that, even in the embryo, the auxin-cytokinin interaction may act to define distinct spatial domains rather than a specific embryonic cell. Supporting this view is the *han* mutant, in which a proximal shift in the auxin domain triggers an ectopic formation of a new root at the new auxin boundary, making a specific cellular morphology dispensable for embryonic root formation (Nawy et al., 2010). Indeed, in

many regeneration systems, the newly replaced organs exhibit flexibility in scale in order to match the size of the remnant body parts (Oviedo et al., 2003). While genetic modifiers may be required to adapt patterning programs from the small embryo to the larger adult root (Moreno-Risueno et al., 2015), our results suggest that the plant can generate a root on different scales, using hormone domains as a common patterning mechanism.

### A Model for Root Patterning during Early Ontogeny

Tissue identities in the reformed meristem appear to be established separately from the activity of the stem cell niche. While stem cells generated new files from the inside out, cell identities all recovered in an outside-in manner. One possibility is that these dynamics reflect a “top-down” flow of cell fate information through cell-to-cell communication (van den Berg et al., 1995). However, cell identity was closely correlated with hormone domain formation, and the position of the root cap boundary and the convergence of radial files could be altered with the manipulation of auxin and cytokinin levels. Given the mutual antagonism between these hormones (Bishopp et al., 2011), an attractive hypothesis is that the tendency of auxin and cytokinin to form complementary but juxtaposed domains could be used to position the root cap, internal root tissues, and the stem cell niche in multiple contexts of root formation (**Figure 7**). Indeed, similar self-organizing auxin-cytokinin interactions provide positional information in other patterning processes in the plant (Bielach et al., 2012; Bishopp et al., 2011; Chang et al., 2015; De Rybel et al., 2014).

It has been shown that mutants defective in pericycle activity and lateral root initiation are also inhibited in some aspects of regeneration (Liu et al., 2014; Sugimoto et al., 2010), but, as shown here, not in root meristem regeneration, demonstrating that regeneration is not absolutely dependent on lateral root programs. Pericycle may be a common source of regenerative tissue, but we posit that many cells capable of dividing can form a minimal field of competent cells in which juxtaposed auxin-cytokinin domains serve as positional guides.

### The Robustness of Pattern and Developmental Plasticity

Our single-cell analyses showed that identity transitions are extremely rapid in plants, as early as 3 hr after injury. Still, despite this plasticity, plant organs are able to maintain robust patterns over long periods of time. How can this contrast between highly responsive organ reorganization and stable organ patterning be reconciled?

Several mechanisms can explain this patterning stability, such as chromatin modifications that limit the cell’s developmental potential (Ikeuchi et al., 2015). Importantly, feedback loops between auxin and cytokinin (Bishopp et al., 2011) and between patterning genes and hormonal pathways have been identified, such as the stele-localized transcription factor *PHABULOSA*, which activates cytokinin synthesis (Dello Ioio et al., 2012), and *SHR*, which activates cytokinin degradation in the surrounding endodermis (Kurakawa et al., 2007).

Indeed, spatial patterning is strongly buffered during steady-state development, as we observed only mild effects when hormonal treatment was applied to intact meristems or to meristems at later stages of regeneration. However, root injury

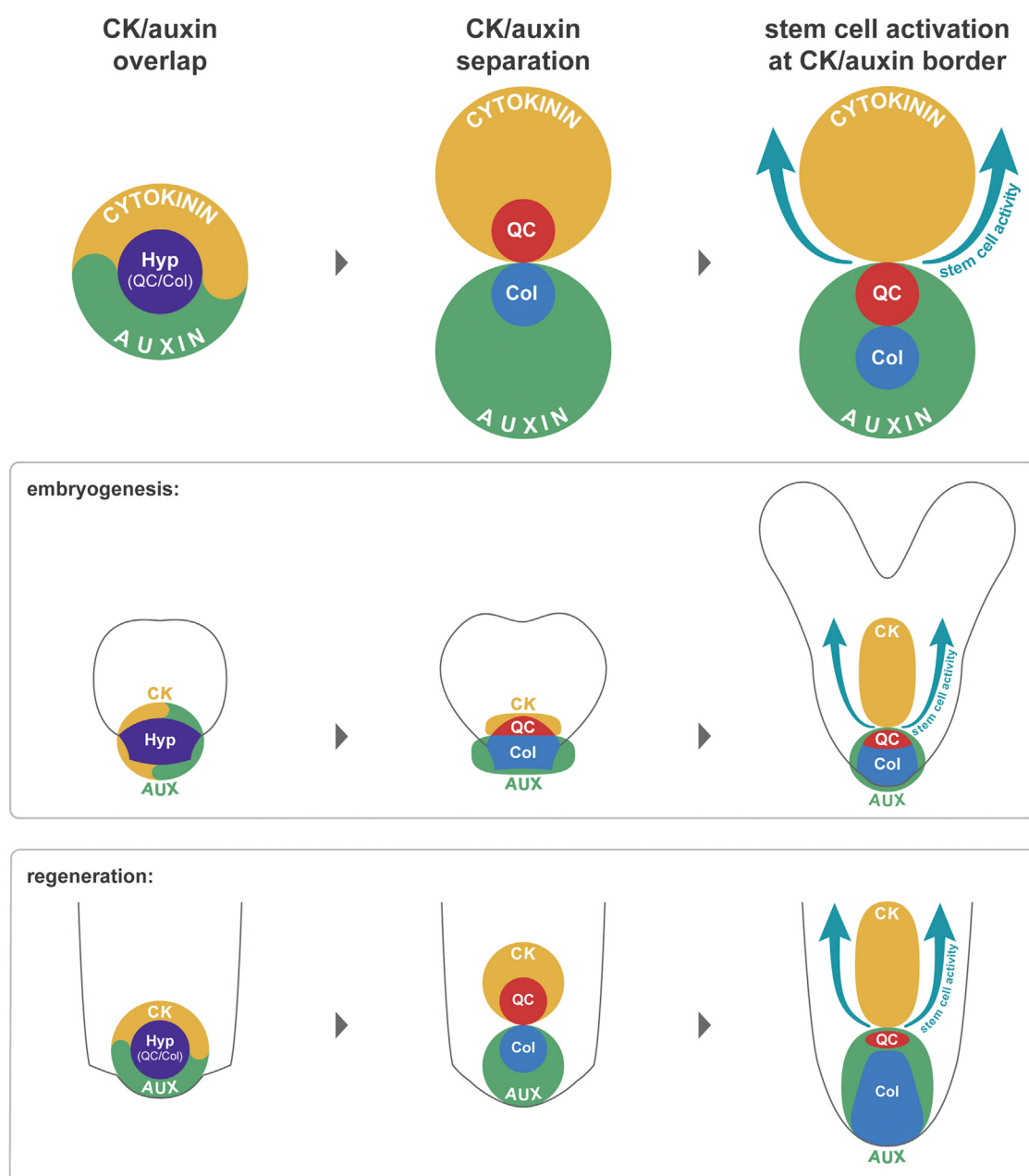


**Figure 7. A General Model for Root Regeneration**

Similar to embryonic root development, regeneration initiates with a transient overlap of auxin (Aux) and cytokinin (CK) signaling, which then separates to a proximal cytokinin and a distal auxin domain, providing spatial cues for the root cap, stem cell niche, and proximal identities. Col, columella; Hyp, hypophysis.

appears to disrupt these stabilizing feedbacks, providing a transient opportunity for hormone signaling to reset tissue boundaries. Accordingly, hormone treatments in the early stages of regeneration could alter major landmarks of the root, such as the extent of the cap and the position of the stem cell niche. The transient destabilization of feedback mechanisms that normally maintain stable patterns in the adult meristem would allow scalable, embryo-like programs to replay during permissive developmental windows, such as instigated by injury.

## EXPERIMENTAL PROCEDURES

### Plant Growth, Imaging, and Regeneration Assay

Plants were grown as previously described (Efroni et al., 2015). Mutant alleles of *jkd-4*, *nww*, and *mp-S319* were previously characterized (Crawford et al., 2015; Hassan et al., 2010; Schlereth et al., 2010). Regeneration assays were performed as described by Sena et al. (2009). For hormonal treatment, root tips were cut at 80 µm above the QC, moved to agar plates (1/2 Murashige and Skoog [MS] medium, 0.5% sucrose, 0.8% agar, [pH 5.7]) containing 2,4-D (2,4-dichlorophenoxyacetic acid; Sigma), BAP (6-benzylamino purine;

Sigma), or both and placed vertically in a growth chamber for recovery. For confocal imaging, seedlings were stained with propidium iodide (10 µg/ml), mounted in water, and visualized using either Leica SPE or Leica SP5 confocal microscopes. For live imaging, cut roots of plants carrying either the lineage marker or the histone marker 35S:H2B-mCherry were placed between a coverslip and an agar block and imaged using an inverted Leica TCS SPE with inverted confocal at fixed intervals (see also [Supplemental Experimental Procedures](#)).

#### Clonal Analysis

The inducible tissue-specific lineage lines for SCR, AHP6, and A14 were constructed following the protocols described previously ([Efroni et al., 2015](#)). To induce clones, seedlings 5 days after germination (DAG) were placed on agar plates containing 15 µm dexamethasone (Sigma) for 24 hr followed by inspection under a fluorescent microscope. Root tips of uniformly induced plants were cut, and plants were moved to agar plates, placed vertically for recovery, and imaged at specified intervals.

#### Single-Cell RNA-Seq and Bioinformatic Analysis

Cells were isolated from cut roots using a short (1- to 2-hr) cell-wall digestion, followed by three filtrations through a 40-µm screen. CFP-positive protoplasts were sorted using FACS (fluorescence-activated cell sorting; either BD Aria or Sony SY3200) into 96-well plates containing lysis buffer using gates to ensure a single cell per droplet ([Figures S7A and S7B](#)). Single cells were subject to cDNA synthesis, amplification, library preparation, read alignment, and expression calling ([Supplemental Experimental Procedures](#)). To derive cell-identity scores, marker Spec scores were calculated as described previously ([Efroni et al., 2015](#)), and 579 tissue markers selected, checking first whether read depth affected cell-identity or mixed-identity calls ([Figures S7C and S7D](#)). To determine background ICI levels, we used ICI scores for QC, Columella, and Epidermis\LR in uncut, stele-derived cells as threshold values ([Figure S7E; Supplemental Experimental Procedures](#)). To produce the multidimensional scaling plot, we used the expression of all 579 identity markers, which were Z-normalized to reduce outlier effects and scaled using the cmdscale function in R.

#### ACCESSION NUMBERS

The accession number for the RNA-seq data reported in this paper is GEO: GSE74488.

#### SUPPLEMENTAL INFORMATION

Supplemental Information includes Supplemental Experimental Procedures, seven figures, three tables, and one movie and can be found with this article online at <http://dx.doi.org/10.1016/j.cell.2016.04.046>.

#### AUTHOR CONTRIBUTIONS

Conceptualization, I.E., A.M., T.N., and K.D.B.; Methodology, I.E., T.N., R.R., R.S., and K.D.B.; Software, I.E.; Investigation, I.E., A.M., P.-L.I., R.R., N.D., and A.P.; Resources, R.S.; Writing, I.E., T.N., and K.D.B.; Visualization (Graphical Abstract, [Figure 7](#)), R.R.; Supervision, I.E. and K.D.B.

#### ACKNOWLEDGMENTS

We thank Charles W. Melnyk and Bruno Müller for sharing materials; Claude Desplan, Esteban Mazzoni, Phillip Benfey, Kim Gallagher, and Wolfgang Lukowitz for critical reading of this manuscript; and the NYU GenCore for generating RNA-seq data. Funding was provided by NIH grant R01 GM078279 to K.D.B. and EMBO grant LTF185-2010 for I.E.

Received: November 4, 2015

Revised: March 2, 2016

Accepted: April 14, 2016

Published: May 19, 2016

#### REFERENCES

- Aida, M., Beis, D., Heidstra, R., Willemsen, V., Blilou, I., Galinha, C., Nusse, L., Noh, Y.S., Armasino, R., and Scheres, B. (2004). The PLETHORA genes mediate patterning of the *Arabidopsis* root stem cell niche. *Cell* 119, 109–120.
- Atta, R., Laurens, L., Boucheron-Dubuisson, E., Guivarc'h, A., Carnero, E., Giraudat-Pautot, V., Rech, P., and Chiriqui, D. (2009). Pluripotency of *Arabidopsis* xylem pericycle underlies shoot regeneration from root and hypocotyl explants grown in vitro. *Plant J.* 57, 626–644.
- Bellini, C., Pacurar, D.I., and Perrone, I. (2014). Adventitious roots and lateral roots: similarities and differences. *Annu. Rev. Plant Biol.* 65, 639–666.
- Bennett, T., and Scheres, B. (2010). Root development—two meristems for the price of one? *Curr. Top. Dev. Biol.* 91, 67–102.
- Berleth, T., and Jürgens, G. (1993). The role of the MONOPTEROS gene in organising the basal body region of the *Arabidopsis* embryo. *Development* 118, 575–587.
- Bielach, A., Podlesakova, K., Marhavy, P., Duclercq, J., Cuesta, C., Muller, B., Grunewald, W., Tarkowski, P., and Benkova, E. (2012). Spatiotemporal regulation of lateral root organogenesis in *Arabidopsis* by cytokinin. *Plant Cell* 24, 3967–3981.
- Birnbaum, K.D., and Sánchez Alvarado, A. (2008). Slicing across kingdoms: regeneration in plants and animals. *Cell* 132, 697–710.
- Birnbaum, K.D., and Kussell, E. (2011). Measuring cell identity in noisy biological systems. *Nucleic Acids Res.* 39, 9093–9107.
- Bishopp, A., Help, H., El-Shour, S., Weijers, D., Scheres, B., Friml, J., Benková, E., Mähönen, A.P., and Helariutta, Y. (2011). A mutually inhibitory interaction between auxin and cytokinin specifies vascular pattern in roots. *Curr. Biol.* 21, 917–926.
- Chang, L., Ramireddy, E., and Schmülling, T. (2015). Cytokinin as a positional cue regulating lateral root spacing in *Arabidopsis*. *J. Exp. Bot.* 66, 4759–4768.
- Chapman, E.J., and Estelle, M. (2009). Mechanism of auxin-regulated gene expression in plants. *Annu. Rev. Genet.* 43, 265–285.
- Chen, Y., Love, N.R., and Amaya, E. (2014). Tadpole tail regeneration in *Xenopus*. *Biochem. Soc. Trans.* 42, 617–623.
- Crawford, B.C.W., Sewell, J., Golembeski, G., Roshan, C., Long, J.A., and Yanofsky, M.F. (2015). Plant development. Genetic control of distal stem cell fate within root and embryonic meristems. *Science* 347, 655–659.
- De Rybel, B., Adibi, M., Breda, A.S., Wendrich, J.R., Smit, M.E., Novák, O., Yamaguchi, N., Yoshida, S., Van Isterdael, G., Palovaara, J., et al. (2014). Plant development: Integration of growth and patterning during vascular tissue formation in *Arabidopsis*. *Science* 345, 1255215.
- De Smet, I., Lau, S., Voss, U., Vanneste, S., Benjamins, R., Rademacher, E.H., Schlereth, A., De Rybel, B., Vassileva, V., Grunewald, W., et al. (2010). Bimodal auxin response controls organogenesis in *Arabidopsis*. *Proc. Natl. Acad. Sci. USA* 107, 2705–2710.
- Dello Ilio, R., Galinha, C., Fletcher, A.G., Grigg, S.P., Molnar, A., Willemsen, V., Scheres, B., Sabatini, S., Baulcombe, D., Maini, P.K., and Tsiantis, M. (2012). A PHABULOSA/cytokinin feedback loop controls root growth in *Arabidopsis*. *Curr. Biol.* 22, 1699–1704.
- Efroni, I., Ip, P.-L., Nawy, T., Mello, A., and Birnbaum, K.D. (2015). Quantification of cell identity from single-cell gene expression profiles. *Genome Biol.* 16, 9.
- Feldman, L.J. (1976). The de novo origin of the quiescent center regenerating root apices of *Zea mays*. *Planta* 128, 207–212.
- Friml, J., Vieten, A., Sauer, M., Weijers, D., Schwarz, H., Hamann, T., Offringa, R., and Jürgens, G. (2003). Efflux-dependent auxin gradients establish the apical-basal axis of *Arabidopsis*. *Nature* 426, 147–153.
- Fukaki, H., Tameda, S., Masuda, H., and Tasaka, M. (2002). Lateral root formation is blocked by a gain-of-function mutation in the SOLITARY-ROOT/IAA14 gene of *Arabidopsis*. *Plant J.* 29, 153–168.

- Haecker, A., Gross-Hardt, R., Geiges, B., Sarkar, A., Breuninger, H., Herrmann, M., and Laux, T. (2004). Expression dynamics of WOX genes mark cell fate decisions during early embryonic patterning in *Arabidopsis thaliana*. *Development* 131, 657–668.
- Hamann, T., Mayer, U., and Jürgens, G. (1999). The auxin-insensitive *bodenlos* mutation affects primary root formation and apical-basal patterning in the *Arabidopsis* embryo. *Development* 126, 1387–1395.
- Hamann, T., Benkova, E., Bärle, I., Kientz, M., and Jürgens, G. (2002). The *Arabidopsis BODENLOS* gene encodes an auxin response protein inhibiting MONOPTEROS-mediated embryo patterning. *Genes Dev.* 16, 1610–1615.
- Hardtke, C.S., and Berleth, T. (1998). The *Arabidopsis* gene MONOPTEROS encodes a transcription factor mediating embryo axis formation and vascular development. *EMBO J.* 17, 1405–1411.
- Hassan, H., Scheres, B., and Bilou, I. (2010). JACKDAW controls epidermal patterning in the *Arabidopsis* root meristem through a non-cell-autonomous mechanism. *Development* 137, 1523–1529.
- Heisler, M.G., Ohno, C., Das, P., Sieber, P., Reddy, G.V., Long, J.A., and Meyerowitz, E.M. (2005). Patterns of auxin transport and gene expression during primordium development revealed by live imaging of the *Arabidopsis* inflorescence meristem. *Curr. Biol.* 15, 1899–1911.
- Helariutta, Y., Fukaki, H., Wysocka-Diller, J., Nakajima, K., Jung, J., Sena, G., Hauser, M.T., and Benfey, P.N. (2000). The SHORT-ROOT gene controls radial patterning of the *Arabidopsis* root through radial signaling. *Cell* 101, 555–567.
- Heyman, J., Cools, T., Vandenbussche, F., Heyndrickx, K.S., Van Leene, J., Vercauteren, I., Vanderauwera, S., Vandepoele, K., De Jaeger, G., Van Der Straeten, D., and De Veylder, L. (2013). ERF115 controls root quiescent center cell division and stem cell replenishment. *Science* 342, 860–863.
- Ikeuchi, M., Iwase, A., Rymen, B., Harashima, H., Shibata, M., Ohnuma, M., Breuer, C., Morao, A.K., de Lucas, M., De Veylder, L., et al. (2015). PRC2 represses dedifferentiation of mature somatic cells in *Arabidopsis*. *Nat. Plants* 1, 15089.
- Kareem, A., Durgaprasad, K., Sugimoto, K., Du, Y., Pulianmackal, A.J., Trivedi, Z.B., Abhayadev, P.V., Pinon, V., Meyerowitz, E.M., Scheres, B., and Prasad, K. (2015). PLETHORA genes control regeneration by a two-step mechanism. *Curr. Biol.* 25, 1017–1030.
- Kidner, C., Sundaresan, V., Roberts, K., and Dolan, L. (2000). Clonal analysis of the *Arabidopsis* root confirms that position, not lineage, determines cell fate. *Planta* 211, 191–199.
- Kikuchi, K., Holdway, J.E., Werdich, A.A., Anderson, R.M., Fang, Y., Egnaczyk, G.F., Evans, T., Macrae, C.A., Stainier, D.Y., and Poss, K.D. (2010). Primary contribution to zebrafish heart regeneration by gata4(+) cardiomyocytes. *Nature* 464, 601–605.
- Kurakawa, T., Ueda, N., Maekawa, M., Kobayashi, K., Kojima, M., Nagato, Y., Sakakibara, H., and Kyozuka, J. (2007). Direct control of shoot meristem activity by a cytokinin-activating enzyme. *Nature* 445, 652–655.
- Lavenus, J., Goh, T., Roberts, I., Guyomarc'h, S., Lucas, M., De Smet, I., Fukaki, H., Beeckman, T., Bennett, M., and Laplaze, L. (2013). Lateral root development in *Arabidopsis*: fifty shades of auxin. *Trends Plant Sci.* 18, 450–458.
- Lee, M.M., and Schiefelbein, J. (1999). WEREWOLF, a MYB-related protein in *Arabidopsis*, is a position-dependent regulator of epidermal cell patterning. *Cell* 99, 473–483.
- Lee, J.-Y., Colinas, J., Wang, J.Y., Mace, D., Ohler, U., and Benfey, P.N. (2006). Transcriptional and posttranscriptional regulation of transcription factor expression in *Arabidopsis* roots. *Proc. Natl. Acad. Sci. USA* 103, 6055–6060.
- Lin, Y., and Schiefelbein, J. (2001). Embryonic control of epidermal cell patterning in the root and hypocotyl of *Arabidopsis*. *Development* 128, 3697–3705.
- Liu, J., Sheng, L., Xu, Y., Li, J., Yang, Z., Huang, H., and Xu, L. (2014). WOX11 and 12 are involved in the first-step cell fate transition during de novo root organogenesis in *Arabidopsis*. *Plant Cell* 26, 1081–1093.
- Mähönen, A.P., Bonke, M., Kauppinen, L., Riikonen, M., Benfey, P.N., and Helariutta, Y. (2000). A novel two-component hybrid molecule regulates vascular morphogenesis of the *Arabidopsis* root. *Genes Dev.* 14, 2938–2943.
- Mayer, U., Büttner, G., and Jürgens, G. (1993). Apical-basal pattern formation in the *Arabidopsis* embryo: studies on the role of the *gnom* gene. *Development* 17, 149–162.
- Moreno-Risueno, M.A., Sozzani, R., Yardimci, G.G., Petricka, J.J., Vernoux, T., Bilou, I., Alonso, J., Winter, C.M., Ohler, U., Scheres, B., and Benfey, P.N. (2015). Transcriptional control of tissue formation throughout root development. *Science* 350, 426–430.
- Müller, B., and Sheen, J. (2008). Cytokinin and auxin interaction in root stem-cell specification during early embryogenesis. *Nature* 453, 1094–1097.
- Nawy, T., Lee, J.-Y., Colinas, J., Wang, J.Y., Thongrod, S.C., Malamy, J.E., Birnbaum, K., and Benfey, P.N. (2005). Transcriptional profile of the *Arabidopsis* root quiescent center. *Plant Cell* 17, 1908–1925.
- Nawy, T., Bayer, M., Mravec, J., Friml, J., Birnbaum, K.D., and Lukowitz, W. (2010). The GATA factor HANABA TARANU is required to position the proembryo boundary in the early *Arabidopsis* embryo. *Dev. Cell* 19, 103–113.
- Okushima, Y., Fukaki, H., Onoda, M., Theologis, A., and Tasaka, M. (2007). ARF7 and ARF19 regulate lateral root formation via direct activation of LBD/ASL genes in *Arabidopsis*. *Plant Cell* 19, 118–130.
- Oviedo, N.J., Newmark, P.A., and Sánchez Alvarado, A. (2003). Allometric scaling and proportion regulation in the freshwater planarian Schmidtea mediterranea. *Dev. Dyn.* 226, 326–333.
- Rademacher, E.H., Lokerse, A.S., Schlereth, A., Llavata-Peris, C.I., Bayer, M., Kientz, M., Freire Rios, A., Borst, J.W., Lukowitz, W., Jürgens, G., and Weijers, D. (2012). Different auxin response machineries control distinct cell fates in the early plant embryo. *Dev. Cell* 22, 211–222.
- Roensch, K., Tazaki, A., Chara, O., and Tanaka, E.M. (2013). Progressive specification rather than intercalation of segments during limb regeneration. *Science* 342, 1375–1379.
- Sabatini, S., Beis, D., Wolkenfelt, H., Murfett, J., Guilfoyle, T., Malamy, J., Benfey, P., Leyser, O., Bechtold, N., Weisbeek, P., and Scheres, B. (1999). An auxin-dependent distal organizer of pattern and polarity in the *Arabidopsis* root. *Cell* 99, 463–472.
- Sabatini, S., Heidstra, R., Wildwater, M., and Scheres, B. (2003). SCARECROW is involved in positioning the stem cell niche in the *Arabidopsis* root meristem. *Genes Dev.* 17, 354–358.
- Sánchez Alvarado, A., and Tsionis, P.A. (2006). Bridging the regeneration gap: genetic insights from diverse animal models. *Nat. Rev. Genet.* 7, 873–884.
- Satija, R., Farrell, J.A., Gennert, D., Schier, A.F., and Regev, A. (2015). Spatial reconstruction of single-cell gene expression data. *Nat. Biotechnol.* 33, 495–502.
- Schaller, G.E., Bishopp, A., and Kieber, J.J. (2015). The yin-yang of hormones: cytokinin and auxin interactions in plant development. *Plant Cell* 27, 44–63.
- Scheres, B.J.G., Wolkenfelt, H., Willemse, V., Terlouw, M., Lawson, E., Dean, C., and Weisbeek, P. (1994). Embryonic origin of the *Arabidopsis* primary root and root meristem initials. *Development* 120, 2475–2487.
- Schlereth, A., Möller, B., Liu, W., Kientz, M., Flipse, J., Rademacher, E.H., Schmid, M., Jürgens, G., and Weijers, D. (2010). MONOPTEROS controls embryonic root initiation by regulating a mobile transcription factor. *Nature* 464, 913–916.
- Sena, G., Wang, X., Liu, H.-Y., Hofhuis, H., and Birnbaum, K.D. (2009). Organ regeneration does not require a functional stem cell niche in plants. *Nature* 457, 1150–1153.
- Skoog, F., and Miller, C.O. (1957). Chemical regulation of growth and organ formation in plant tissues cultured in vitro. *Symp. Soc. Exp. Biol.* 11, 118–130.
- Sugimoto, K., Jiao, Y., and Meyerowitz, E.M. (2010). *Arabidopsis* regeneration from multiple tissues occurs via a root development pathway. *Dev. Cell* 18, 463–471.

- Sugimoto, K., Gordon, S.P., and Meyerowitz, E.M. (2011). Regeneration in plants and animals: dedifferentiation, transdifferentiation, or just differentiation? *Trends Cell Biol.* **21**, 212–218.
- ten Hove, C.A., Lu, K.-J., and Weijers, D. (2015). Building a plant: cell fate specification in the early *Arabidopsis* embryo. *Development* **142**, 420–430.
- To, J.P.C., Haberer, G., Ferreira, F.J., Deruère, J., Mason, M.G., Schaller, G.E., Alonso, J.M., Ecker, J.R., and Kieber, J.J. (2004). Type-A *Arabidopsis* response regulators are partially redundant negative regulators of cytokinin signaling. *Plant Cell* **16**, 658–671.
- Ueda, M., Zhang, Z., and Laux, T. (2011). Transcriptional activation of *Arabidopsis* axis patterning genes WOX8/9 links zygote polarity to embryo development. *Dev. Cell* **20**, 264–270.
- van den Berg, C., Willemse, V., Hage, W., Weisbeek, P., and Scheres, B. (1995). Cell fate in the *Arabidopsis* root meristem determined by directional signalling. *Nature* **378**, 62–65.
- Welch, D., Hassan, H., Blilou, I., Immink, R., Heidstra, R., and Scheres, B. (2007). *Arabidopsis JACKDAW* and *MAGPIE* zinc finger proteins delimit asymmetric cell division and stabilize tissue boundaries by restricting SHORT-ROOT action. *Genes Dev.* **21**, 2196–2204.
- Wendrich, J.R., Möller, B.K., Uddin, B., Radoeva, T., Lokerse, A.S., De Rybel, B., and Weijers, D. (2015). A set of domain-specific markers in the *Arabidopsis* embryo. *Plant Reprod.* **28**, 153–160.
- Wysocka-Diller, J.W., Helariutta, Y., Fukaki, H., Malamy, J.E., and Benfey, P.N. (2000). Molecular analysis of SCARECROW function reveals a radial patterning mechanism common to root and shoot. *Development* **127**, 595–603.
- Xu, J., Hofhuis, H., Heidstra, R., Sauer, M., Friml, J., and Scheres, B. (2006). A molecular framework for plant regeneration. *Science* **311**, 385–388.
- Zürcher, E., Tavor-Deslex, D., Lituiev, D., Enkerli, K., Tarr, P.T., and Müller, B. (2013). A robust and sensitive synthetic sensor to monitor the transcriptional output of the cytokinin signaling network in planta. *Plant Physiol.* **161**, 1066–1075.